Cross-talk between Hippo and Wnt signalling pathways in intestinal crypts: insights from an agent-based model.

Daniel Ward[1], Alexander G. Fletcher[2,3], Martin Homer[1,^,+], Lucia Marucci[1,4,^5,+]

[1]Department of Engineering Mathematics, University of Bristol, BS8 1UB, UK; [2]School of Mathematics and Statistics, University of Sheffield, Sheffield, S3 7RH, UK; [3]Bateson Centre, University of Sheffield, Sheffield, S10 2TN, UK; [4]BrisSynBio, University of Bristol, Bristol, BS8 1TQ, UK; [5]School of Cellular and Molecular Medicine, University of Bristol, Bristol, BS8 1TD, UK.

^ These authors share senior authorship

[+] Corresponding authors: Dr Martin Homer (martin.homer@bristol.ac.uk); Dr Lucia Marucci (lucia.marucci@bristol.ac.uk)

Abstract

Intestinal crypts are responsible for the total cell renewal of the lining of the intestines, occurring every 4-7 days in humans. This rapid turnover is governed by the complex interplay between signalling pathways and the cell cycle within individual cells in the crypts. The role of Wnt signalling in governing cell proliferation and differentiation in the intestinal crypt has been extensively studied, with increased signalling found towards the lower regions of the crypt. Recent studies have shown that the Wnt signalling gradient found within the crypt may arise as a result of division-based spreading from a Wnt 'reservoir' at the crypt base. The discovery of the Hippo pathway's involvement in maintaining crypt homeostasis is more recent; a mechanistic understanding of Hippo pathway dynamics, and its possible cross-talk with the Wnt pathway, remains lacking. To explore how the interplay between these pathways may control crypt homeostasis and dysplasia we developed and analysed a mathematical model coupling an ordinary differential equation description of Wnt and Hippo signalling with a cell-based description of cell movement, proliferation and contact inhibition. Furthermore, we compared an imposed Wnt gradient with a division-based Wnt gradient model. Our results suggest that Hippo signalling affects the Wnt pathway by reducing the presence of free cytoplasmic β-catenin, causing cell cycle arrest. This process slows the rate of crypt turnover, previously attributed only to mutations in Wnt pathway components commonly observed in colorectal cancers. We also show that a division-based spreading of Wnt can form a Wnt gradient, resulting in proliferative dynamics comparable to imposed-gradient models. This suggests that imposed-gradient models are a reasonable approximation of experimentally observed Wnt gradients, however they provide little insight into the source of Wnt. Finally, a simulated APC double mutant, with misregulated Wnt and Hippo signalling activity, is predicted to be capable of completing a more rapid monoclonal conversion of the crypt than a Wnt-only mutant.

Author summary

Colorectal cancer is the fourth leading cause of cancer death worldwide. It is generally established that colorectal cancer occurs upon disruption of the dynamics of crypts, tubular indentations lining the walls of the gastrointestinal tract that are responsible for renewal of the intestinal epithelium. Thus, understanding the mechanisms that regulate intestinal crypt dynamics is instrumental to understand how colorectal cancer can emerge. We used mathematical modelling to explore how crypt dynamics emerge from the interactions across several biological scales, including mutations that cause an abnormal cell response to changes at the cell or tissue level, cell proliferation and motility within the crypt. Our model describes, in each cell within the crypt, levels and dynamics of genes involved in two signalling pathways – the canonical Wnt and Hippo pathways – relevant for cell proliferation and adhesion. In simulations, we predict how the crosstalk between these pathways affects crypt dynamics in both healthy and dysplastic cases. Furthermore, our simulations match recent biological evidence of a novel mechanism, based on cell division, causing heterogeneous and graded localisation of different cell types (dividing or not) within the crypt. Our results suggest the possibility of combined disease treatment, targeting both the Wnt and Hippo pathways.

Introduction

Colorectal cancer is the third most common malignant cancer, and the fourth leading cause of cancer death worldwide, accounting for roughly 1.4 million new cases and approximately 700,000 deaths in 2012 (1). Although the overall mortality rate for colorectal cancer has been declining by roughly 2% per year between 1997 and 2007 in the EU, from 19.7 to 17.4/100,000 men and from 12.5 to 10.5/100,000 women (2), mainly due to improved early diagnosis and/or an improved lifestyle, colorectal cancer still affects a significant number of people worldwide. Improvement of these statistics (through, for example, new diagnostics and treatment) will depend on a better understanding of the cellular mechanisms that are responsible for the disease. It has been suggested that there are specific cancer stem cells that develop and propagate colorectal cancer (3) . Within the intestine, stem cells reside within crypts, tubular indentations lining the walls of the gastrointestinal tract (4) that are responsible for the total cell renewal of the intestine lining every 4-7 days in humans (5-7) (more rapidly in mice (8)). In a healthy crypt, regulatory networks tightly control individual cell and crypt homeostasis, through multi-level processes such as proliferation, cell adhesion, growth factors and production of other secreted molecules. Changes to these underlying regulatory networks due to mutations can disrupt crypt dynamics and eventually result in tumorigenesis. Of particular significance are the Wingless/Int (Wnt) and Hippo signalling pathways.

The role of the canonical Wnt signalling pathway (i.e. the Wnt/β-catenin pathway, hereinafter referred to as Wnt pathway) in regulating the expression of target genes linked to proliferation and differentiation has been extensively studied, both experimentally and theoretically (9-12). Within the gastrointestinal tract, it is known that Wnt signalling governs proliferative dynamics specific to the lower regions of intestinal crypts (13). The importance of the Wnt pathway in maintaining a healthy cell turnover is clear from studies reporting consequences of Wnt signalling dysfunction (13-16), with the development of intestinal tumours and polyps linked to mutations in the signalling pathway cascade, and approximately 80% of all human colon tumours reported to show mutations that inactivate the APC gene (17). The main cellular effect of activation of the Wnt signalling pathway is to alter the subcellular localisation of β-catenin (9, 15). In the absence of a Wnt signal ('Wnt-Off'),

102 cytoplasmic β-catenin is rapidly degraded by the destruction complex formed by APC, Axin, Ser/Thr
103 kinases GSK-3 and CK1 (9). In the presence of a Wnt signal ('Wnt-On'), extracellular Wnt ligands
104 bind to Frizzled cell surface receptors, causing inhibition of the destruction complex via sequestration
105 of β-catenin. This leads to the accumulation of unphosphorylated β-catenin in the cytoplasm and thus
106 increased shuttling of β-catenin to the nucleus, where it binds to TCF/LEF transcription factors and
107 activates expression of Wnt target genes, many of which regulate cell proliferative dynamics (10).
108 Typically, malignant transformations of cells within the crypt involve mutations in the APC gene
109 (18), causing aberrant build-up of β-catenin and expression of Wnt target genes (10, 11, 14, 19). Cell
110 proliferation occurs predominantly in the bottom third of the crypt (20), with a low level of
111 extracellular Wnt detected at the crypt orifice and a maximal level at the base (14, 15, 21). Previous
112 studies have suggested that such a Wnt gradient helps maintain crypt homeostasis (specifically,
113 constancy in the numbers of different cell types, and overall crypt size), determines subcellular β-
114 catenin localisation and kinetics and, ultimately, regulates cell-cycle dynamics (22, 23). Indeed, many
115 theoretical models of crypt dynamics have linked an imposed Wnt gradient directly to cell-cycle
116 duration (5, 24-26). However, more recent experimental data suggest that the Wnt gradient results
117 from a cellular division-based spreading of Wnt from the base of the crypt, where there is an effective
118 reservoir of Wnt, and consequent Wnt dilution throughout the crypt (27).

119 Aside from Wnt signalling, other processes and signalling pathways also play important roles
120 in crypt homeostasis. For example, contact inhibition (CI) of cell proliferation is defined as the
121 cessation of cell-cycle progression due to contact with other cells, leading to a transition to a dense
122 monolayer of epithelial cells (28). Increased CI can be due to forced reduction in cell volume,
123 externally applied stress, or increase in the cell density, with solid stress shown to inhibit the growth
124 of cell spheroids *in vitro*, regardless of differentiation state (29). Overcrowding can also induce live
125 cell extrusion from the monolayer (30), however, with regards to crypt homeostasis, this appears to
126 occur towards the crypt orifice, thus beyond the region we would expect proliferative cells to reside.
127 We consider CI in our investigation, as the precise nature of the mechanisms driving it, possibly

including the interplay of signalling pathways regulating crypt homeostasis, are not well understood (31, 32).

It has been suggested that the Hippo signalling pathway, which is deregulated in multiple cancers (33, 34), plays a role in preventing cell proliferation due to CI (35), with signalling linked to the volume of a cell and the overall stress applied to it (35-37). The Hippo pathway negatively regulates Yes-associated protein (YAP) and the transcriptional co-activator PDZ-binding motif (TAZ); the activation of YAP and TAZ promotes cell proliferation and inhibits cell death (28, 32). The Hippo pathway restricts the availability and functionality of YAP in the nucleus by altering its level and distribution (31, 38). Over-expression of YAP or its over-activation by Hippo pathway mutations have been shown to counter the effects of CI *in vitro* and organ size control *in vivo*, promoting tissue overgrowth and cancer development (32, 33). The Hippo signalling pathway, unlike other signalling cascades, does not appear to have its own dedicated extracellular peptides and receptors, but instead relies on regulation by a network of upstream components and mechanisms, such as cell polarity complexes and adherens junctions (39). It has been suggested that the Hippo pathway is regulated by the cellular architecture and the mechanical properties of cell environment, possibly serving as a sensor for tissue structure and mechanical tension (36, 40, 41).

Cross-talk between the Hippo and Wnt signalling pathways has been shown to play a key role in mediating cell proliferation (35), by reducing nuclear β-catenin levels and, consequently, the expression of Wnt target genes that control cell-cycle progression. In a Hippo 'off' state, the level of YAP-P remains stable within the cell, and the YAP-P/β-catenin complex remains at minimal levels in the cytoplasm. Conversely, in a Hippo 'on' state there is an increase in YAP-P, which binds to free β-catenin in the cytoplasm creating a YAP-P/β-catenin complex that is unable to localise to the nucleus of the cell, whilst maintaining its membrane bound activities. These results motivate our development of a mathematical model able to capture the mechanisms linking Wnt and Hippo signalling and CI, extending a previously proposed kinetic model of β-catenin within an individual cell (42).

Mathematical modelling has been used to explore crypt dynamics in health and disease, and to better understand how colorectal cancer can emerge from the interactions across several scales of

155 biological processes, such as mutations that cause an abnormal intracellular response to changes at
156 either the cell or tissue levels, and cell proliferation, motility and adhesion (43). Existing
157 mathematical models of crypt dynamics have focussed on Wnt signalling, including its role in
158 monoclonal conversion (the process by which a crypt is populated in its entirety by the progeny of a
159 single ancestor cell (24, 44)), and the effects on subcellular β-catenin localisation on the cell cycle
160 (25). Recently, the possible effects of cell-cycle cessation caused by contact-dependent factors have
161 been investigated by modelling CI as cell-cycle cessation linked to cell volume (5). In all these
162 models, Wnt is assumed to act on cells via an imposed and external gradient. Earlier models assumed
163 that Wnt affects cell-cycle progression dynamically, while a more recent work suggests that cell-cycle
164 duration is dependent on the Wnt signal available immediately after mitosis (5).

165 In what follows, we consider two Wnt models in the multicellular context: the first assumes
166 that Wnt exists as an externally-imposed gradient, with variants as described above, where the Wnt
167 level received by each cell either changes throughout its cell cycle or is updated at the point of each
168 cell division. The second model considers the Wnt level to be an intrinsic property of each individual
169 cell, instead of being prescribed only externally, and hence allows us to test the hypothesis of an
170 emergent Wnt gradient in the crypt. In this second model, Wnt is distributed between the daughter
171 cells following each cell division, with a Wnt source 'reservoir' region located at the base of the crypt.
172 In the case of the small intestine this is akin to the region of Paneth cells that can transfer Wnt to
173 neighbouring cells, although this diffusion has been shown to be limited to 1-2 neighbour cells (27,
174 45). A more recent study has suggested an additional source of Wnt proteins in FOXL1+ telocytes,
175 which form a subepithelial plexus extending from the stomach to the colon, again localised towards
176 the base of the crypt (46).

177 More fundamentally, models of crypt dynamics that explicitly include the Hippo signalling
178 pathway are lacking, preventing a thorough analysis of the effects of Wnt/Hippo crosstalk. To address
179 this, we propose a new model that describes both Hippo and Wnt signalling pathway dynamics, which
180 links their activity to cellular proliferation and CI. We initially consider the effects of Hippo and Wnt
181 at the single-cell level, and analyse their combined role in cell-cycle cessation. Moving to a

182 multicellular framework, we show that crypt dynamics remain fundamentally unaltered upon
183 incorporation of CI via Hippo signalling; the latter, however, plays a crucial role in the monoclonal
184 conversion probabilities upon mutations in Wnt pathway genes.

185

186 **Results**

187 **Intracellular modelling of Wnt/β-catenin and Hippo signalling pathways**

188 We developed an ordinary differential equation (ODE)-based kinetic model to capture the
189 combined effects of Wnt/β-catenin and Hippo signalling on intracellular dynamics. Our model builds
190 on the formalism proposed by van Leeuwen *et al*. (42), which distinguishes adhesive and
191 transcriptional functions of β-catenin. Although alternative models of Wnt signalling exist (47-50),
192 the van Leeuwen formalism was chosen as it incorporates important mechanistic features of the
193 canonical Wnt pathway (including sequestration of β-catenin by the destruction complex, and
194 activation/inactivation of the destruction complex) and couples β-catenin localisation with cell-cycle
195 progression (22). Specifically, when β-catenin localises at the cell membrane, it regulates the
196 formation of E-cadherin-dependent cell-cell contacts, connecting adherens junction proteins to the
197 actin cytoskeleton (42). Accumulation of β-catenin within the cytosol results in its nuclear
198 translocation, activating the transcription of target genes linked to cell-cycle progression and cell-
199 survival. Thus, cytoplasmic β-catenin can either: (a) be sequestered by molecules linked to Wnt gene
200 transcription to form transcriptional complexes, (b) form adhesive complexes at adherens junctions, or
201 (c) undergo Wnt-mediated degradation.

202 We extended the model to include the effect of Hippo on Wnt signalling, to implement cell
203 volume-dependent CI. As postulated by Imajo *et al*. (35), we modelled the Hippo signalling-governed
204 concentration of cytoplasmic phosphorylated YAP to cause a reduction in the levels of nuclear β-
205 catenin. This is in line with experiments showing that Hippo signalling causes increased
206 phosphorylation of YAP, combined with the formation of YAP-P/β-catenin complexes within the cell
207 but constrained to the cytoplasm (31, 34, 35). We assumed that the mechanism of CI is a reduction of

cell volume below the equilibrium volume of a typical crypt epithelial cell, as this should correlate with an increase in surface stress due to cellular crowding in an epithelial monolayer, as well as an increase in cell density (29). We therefore altered the kinetic model to include a volume-dependent nuclear sequestration rate of β-catenin, $\hat{p}_H$ (35), which describes how volume-dependent Hippo signalling decreases the nuclear localisation of β-catenin (thus increasing its cytoplasmic presence without altering its total cellular concentration) and, consequently, cell proliferation dynamics. When the cell volume drops below a threshold the rate $\hat{p}_H$ increases linearly within the range indicated in Table S1.

Figure 1a shows schematically the interplay between Wnt and Hippo signalling in our model, that is the basis for the kinetic diagram in Figure 1b, representing interactions between free axin (X), adhesive molecules (A), the active destruction complex (D), the β-catenin/YAP-P complex (C_H), four molecular forms of β-catenin (C_i, i = A, C, T and U, corresponding to β-catenin contained in the adhesive junction, cytoplasm, transcriptional complexes, and marked for ubiquitination/degradation, respectively), transcriptional molecules (T), and the Wnt target protein (Y).

The temporal Wnt/Hippo dynamics within a single cell were modelled as a system of 10 Ordinary Differential Equations (ODEs, Figure S1); they describe the aforementioned effects of Hippo signalling via the phosphorylated YAP/β-catenin complex, as well as CI effects (details in Supplementary Information). The Wnt/Hippo model is mainly based on mass-action and Hill kinetics (51); it was derived from the original publication (25), and, as such, the parameters were left unchanged in Equations 1-9 where used previously (Figure S1, Table S1). As an extension to the original model, we described the dynamics of the β-catenin/YAP-P complex (C_H, Equation 10, Figure S1) to account for the effects of Hippo signalling on β-catenin localisation; we used again Hill terms, similarly to those in Equations 2 and 7 (Figure S1). The interplay between the Wnt/Hippo signalling and the cell-cycle is governed by the amount of transcriptional β-catenin (C_T); the latter links the signalling ODE model (Figure S1) to the cell-cycle model (ODEs in Figure S2, unchanged from the original work in (25); further details in Supplementary Information).

234 To explore the effect of Hippo signalling on cell-cycle duration and fix the new parameters in
235 the Wnt/Hippo model (Equation 10, Figure S1), we performed a parameter sensitivity analysis,
236 varying the YAP-P/β-catenin complex binding rate ($\hat{p}_H$) and dissociation constant (K_H); these
237 parameters govern the effectiveness of the inhibition of nuclear β-catenin localisation and,
238 consequently, CI. A description of this single-cell analysis is included in the Supplementary
239 Information. The results, shown in Figure 2a, suggest that the saturation coefficient (K_H) has some
240 effect on cell-cycle duration but, more significantly, alters the effective range over which the binding
241 rate ($\hat{p}_H$) controls cell-cycle duration, with changes in the binding rate having the largest effect on
242 delaying and eventually stopping proliferation. We therefore assigned a value to the saturation
243 coefficient K_H (Table S1) which, when combined with Wnt signalling effects on β-catenin
244 localisation, did not cause premature cessation of the cell cycle.

245 We then investigated how the cross-talk between the Hippo and Wnt pathways affects the
246 duration of the cell cycle (*i.e* the time taken for the levels of E2F1 -Equation 2, Figure S2- to surpass
247 the threshold for initiating the transition from the G_1 to the S phase of the cell cycle, as in Swat *et al*
248 (22)). Setting the saturation term K_H to 100nM, to allow for an appropriately sized range over which to
249 vary the binding rate, a concurrent increase in the YAP-P/β-catenin complex binding rate ($\hat{p}_H$), and
250 decrease in Wnt signalling, cause a delay and eventual cessation of the cell cycle (Figure 2b).

251 These results suggest that cells experiencing lower Wnt concentrations are more susceptible
252 to inhibition of proliferation by Hippo signalling as there is less free β-catenin localised in the
253 cytoplasm. This single-cell analysis suggests that the reduction in cytoplasmic β-catenin levels caused
254 by Hippo signalling is able to prevent the progression through the cell cycle, thus inhibiting
255 proliferation.

256 **Multiscale modelling of the intestinal crypt**

257 We incorporated the subcellular Hippo/Wnt ODE model described above into a multiscale
258 model of the intestinal crypt, implemented in Chaste (52, 53), a computational platform previously
259 used to simulate colonic crypt dynamics (5, 24, 25, 44, 54), amongst other multicellular systems (55,

260 56). The modelling of the epithelial cells that make up the intestinal crypt is organised into three
261 interconnected modules: 1. the mechanical model, governing the cell-cell interactions and cell
262 movement; 2. the cell-cycle model, describing how each cell progresses through the G1, S, G2 and M
263 phases, and eventually divides; and 3. a subcellular model, describing the Hippo/Wnt signalling
264 pathway kinetics as in the previous section.

265 We modelled the geometry of the crypt as a cylinder lined with epithelial cells, unrolled to a
266 planar domain with periodic boundary conditions (Figure 2c). We coupled the cell-cycle model to the
267 Wnt/Hippo ODE model (Supplementary Information) to account for CI effects: the YAP-P/β-catenin
268 complex is able to cease cell-cycle progression by decreasing the level of Wnt signalling. To
269 accomplish this, the Hippo signalling module in each cell (i.e. agent) is volume-dependent, and
270 effectively reduces the level of free β-catenin able to localise into the nucleus, activate target genes
271 and ultimately promote cell-cycle progression (Supplementary Information). This mechanism causes a
272 competition between the two pathways: an increase in Wnt shortens the cell cycle, while increasing
273 Hippo signalling lengthens it.

274 We consider two different Wnt models. The first (labelled M1) includes Wnt as an externally-
275 imposed gradient, and has two variants: static (model M1a), in which each cell reads its Wnt signal at
276 birth (5), and dynamic (model M1b), in which each cell continuously updates its Wnt level, as in
277 previous models (24, 25). In the second Wnt model (labelled M2), each cell contains an independent
278 level of Wnt, split with each cell division event between the two daughter cells.

279 **The effects of Hippo and Wnt signalling on wild-type crypt homeostasis**

280 **Wnt Model M1: externally-imposed Wnt gradient, with static (M1a) or dynamic (M1b)**
281 **updating**

282 We investigated, under physiological conditions (i.e. wild type cells), how crypt renewal
283 dynamics are affected by CI and by cross-talk between the Wnt (prescribed as an external gradient;
284 models M1a and M1b) and Hippo pathways by measuring both the mitotic index (i.e., the percentage
285 of cells undergoing mitosis at any given point in time), as a proxy for the proliferative capacity of
286 cells, and the distribution of cell velocities throughout the crypt, to provide a snapshot of crypt

287 motility (Figure 3). We varied two relevant parameters: the CI threshold, and the Wnt level within the
288 crypt. The CI threshold — defined as the cell volume below which the YAP-P/β-catenin complex
289 prevents progression through the cell cycle — is defined as a percentage of the equilibrium cell
290 volume enabling proliferation, and was set to either 60% or 90%; in the latter case, more cells are
291 affected by CI. The Wnt level — defined as the position in the crypt at which the external Wnt
292 gradient reaches its minimum value — is set to either 40% or 100% of the height of the crypt (Figure
293 2c, right panel), as an attempt to account for the proliferative differences of crypts within the small (7,
294 16) and large intestine (8), respectively.

295 The effect of varying Wnt level on mitotic activity (Figure 3a and b) is that, for maximal Wnt
296 level (Figure 3a), the proliferative 'niche' extends further up the crypt than for lower Wnt (Figure 3b);
297 in the latter case, there is a rapid drop-off of mitotic index at approximately 30% of the crypt height.
298 The main difference between the static (M1a) and dynamic (M1b) Wnt models (Figures 3a and b,
299 solid and dashed lines, respectively) is a more rapid drop-off in the mitotic index using the latter
300 approach. This is because updating Wnt level dynamically causes cells to react instantly to changes in
301 the external Wnt level as they move up the crypt, resulting in a more rapid cell-cycle cessation.

302 Varying the threshold volume at which cells are contact-inhibited (Figures 3a and b, red and
303 blue lines corresponding to 60% and 90% of CI threshold, respectively) has a greater effect when cells
304 reach the top of the proliferative niche where the Wnt signal decreases. This result shows that the
305 volume-dependent prevention of β-catenin nuclear localisation, and hence the reduction in mitotic
306 proportion, are more pronounced when there is less free β-catenin to be sequestered. These results
307 match our single-cell simulations, which suggested that the region over which CI is active is reduced
308 with a lower Wnt signal. Also, our crypt simulations indicate that inhibiting the cells at 90% of their
309 equilibrium volume results in a reduction in mitotic activity of approximately 15% at the base of the
310 crypt and of over 40% towards the top of the proliferative 'niche'. This suggests that CI within the
311 crypt is as capable of affecting the proliferative activity of the crypt cells as changing the method of
312 Wnt signalling within the crypt.

313 We checked that our new model, introducing CI, does not dramatically affect the proliferative
314 dynamics in a wild-type crypt when compared to previous models (5, 24, 25). This is confirmed by
315 the results (Figures 3a and b), which suggest that the differential effects of Wnt on proliferation
316 dynamics are greater than those of increasing CI effects.

317 Varying the threshold volume at which cells are contact inhibited from 60% (Figures 3c and
318 d, red boxes) to 90% (Figures 3c and d, blue boxes) of equilibrium volume, results in a reduction in
319 mean crypt velocity of 33%, whilst decreasing the threshold for Wnt from 100% of the crypt to 40%
320 of the crypt (Figures 3c and d, respectively) results in a reduction in mean crypt velocity of 38%. This
321 qualitative similarity is due to the limited effect of CI in a wild type crypt where cells are not, in
322 general, significantly smaller than their expected equilibrium volume.

323 Overall, these agent-based simulations suggest that Wnt signalling levels are the main
324 regulator of cell proliferation within the crypt. Hippo signalling also plays an important role, as
325 Hippo-dependent CI reduces proliferative activity within the crypt, with the largest effects seen in the
326 100% Wnt case, due to the larger number of proliferative cells affected by CI. Considering the two
327 Wnt hypotheses for this externally-imposed Wnt model — static (M1a) and dynamic (M1b) — the
328 reduced mitotic activity in the M1b crypt is not in line with the mitotic activity seen experimentally
329 (6), which suggests that the static (M1a) modelling hypothesis is more physiologically plausible.

330 **Wnt Model M2: cell division-based Wnt**

331 A prescribed and fixed external gradient of Wnt is a feature of existing computational models
332 of crypt dynamics, effectively prescribing a spatial proliferation threshold (5, 24, 25). We modified
333 our model to account for the aforementioned recent experimental results suggesting an alternative,
334 division-based Wnt process (27), and investigated whether this approach could result in an emergent
335 Wnt gradient in the crypt. We therefore set only cells at the base of the crypt to receive a maximal
336 Wnt signal, forming a Wnt reservoir, whose size (as a proportion of the height of the crypt) is a model
337 parameter. It has been shown experimentally that Wnt does not readily diffuse into surrounding
338 cells (27), and we therefore neglected diffusion-based spreading of Wnt. Instead, Wnt is shared

339 stochastically between daughter cells, so that daughter cells contain a proportion $0.5 \pm \xi$ of the mother
340 cell's Wnt level at each division (57), where ξ is a sample from a Normally distributed random
341 variable with zero mean and standard deviation σ (set as a model parameter), appropriately truncated
342 to ensure the proportion remains in the interval [0,1].

343 Initial simulations, carried out with noiseless Wnt allocation on division (i.e. $\sigma = 0$), resulted in
344 emergent Wnt gradients over the crypt domain (Figures 4a, b). Increasing the size of the Wnt
345 reservoir from 10% to 20% of the crypt height reduces the steepness of the resultant Wnt gradient,
346 without affecting the mean Wnt density at the top of the crypt, so that it more closely resembles the
347 imposed linear Wnt gradient of previous models.

348 We then introduced noise in the allocation of Wnt and repeated the wild type crypt *in silico*
349 experiments with 5% (σ=0.05) and 10% (σ=0.1) noise, in both the 10% and 20% Wnt reservoir crypts
350 (Figures 4c, d). The mean Wnt gradient is not strongly affected by the introduction of this division
351 noise, as expected as the mean of the noise added is zero. Mitotic index results (Figures 4c and d)
352 show that, considering division-based spreading of Wnt with no noise (blue lines), there is a reduction
353 followed by a sharp increase in mitotic activity in the region where the first cell division occurs (at
354 approximately 20%/40% of the total height of the crypt, in case of a 10%/20% Wnt reservoir,
355 respectively). When introducing noise in Wnt allocation upon division (Figures 4c and d, red and
356 green lines), this reduction and subsequent increase in mitotic activity is smoothed, better capturing
357 the mitotic activity recorded experimentally (6). The latter results suggest that the distribution of Wnt
358 between daughter cells upon cell division might not be purely symmetric, which has been suggested
359 in a previous study (57). A comparison of externally imposed versus division-based Wnt model
360 simulations (Figures 3a, b and Figures 4c, d, respectively) suggests that a crypt with a 10% Wnt
361 reservoir is representative of a colonic crypt, while a 20% Wnt reservoir can resemble small intestinal
362 crypt dynamics (6, 7). The presence of Paneth cells in the small intestinal crypt could account for this
363 larger required Wnt reservoir that we see in our experiments; conversely, an external Wnt signal that
364 does not extend for the full height of the crypt would also suffice in explaining this larger Wnt
365 presence.

366 **Introducing mutations in both Wnt and Hippo signalling in the crypt**

367 Finally, we investigated the effects of CI on a dysplastic crypt; in this case, there can be a
368 significant increase in cell number due to over-proliferation of mutant cells, resulting in a decrease in
369 cell volume, at which point the effects of CI may play a more significant role. We considered a
370 possible APC double-mutant (58), where there is total disruption of the β-catenin destruction complex
371 (18, 26) as well as disruption to Hippo signalling within the cell (35); as a result, APC double-mutant
372 cells hyper-proliferate throughout the crypt. The mutant has proliferative dynamics independent of
373 both Wnt signal and cell volume. In what follows, we consider only the most realistic imposed
374 external Wnt model (M1a) and the cell division-based Wnt model (M2). We conducted *in silico*
375 experiments, varying the threshold volume at which Hippo signalling is active in the healthy cells,
376 together with the size of the Wnt gradient (in M1a) and of the Wnt reservoir (M2); Figure 5 shows
377 mutant cell washout probabilities (i.e. the likelihood of healthy cells being able to remove the mutant
378 from the crypt) upon insertion in the crypt of one APC double-mutant cell.

379 In the imposed Wnt gradient crypt (M1a, Figure 5a), an increase of the Wnt signal from 40%
380 to 100% of the crypt (Figure 5a, red and blue lines respectively) resulted in only a small change to the
381 washout probability at low levels of CI. Conversely, at the maximal CI volume threshold (90% of
382 equilibrium volume), the washout probability increases from approximately 45% in the 100% Wnt
383 case to 70% in the 40% Wnt case, as the advantage of the mutant cell is reduced due to increase of
384 proliferating healthy cells; recall that only wild type cells are affected by CI, and that mutant cells
385 proliferate independent of cell volume and Wnt level. The increase in level of CI (from 60% to 90%
386 of equilibrium volume) reduces the washout probability by nearly half in the 40% Wnt crypt (Figure
387 5a, red line). It is in this case where the advantage gained by a mutant cell from the combination of its
388 increased proliferative capacity and CI is most significant. The reduction in washout probability is
389 also comparable with previous models, where additional advantage was predicted to be gained by the
390 mutant cell through its increased adhesion to the crypt substrate and to the surrounding cells (24). Of
391 note, we did not model the altered adhesion of mutant cells, to specifically focus on signalling- and
392 volume-dependent CI.

In the division-based Wnt model (M2, Figure 5b), simulations of the same mutant takeover show that, for maximal CI volume (90% of equilibrium volume), an increase in the size of the Wnt reservoir from 10% to 20% of the height of the crypt (Figure 5b, red and blue lines respectively) results in a large increase in the relative washout probability (from approximately 45% to 70%). Decreasing the volume threshold for CI resulted in a smaller decrease in the washout probability of that in the imposed-Wnt-gradient crypt with high Wnt (Figure 5, blue lines), but similar behaviour for low-Wnt (Figure 5, red lines).

Overall, the simulated dysplastic dynamics qualitatively match those predicted by the imposed Wnt gradient model, with a reduction in washout probability resulting from a stronger level of CI, and an increase in washout probability in response to a higher level of Wnt in the crypt.

Discussion

Although the role of the Wnt signalling pathway in governing the proliferative dynamics of cells within intestinal crypts has been extensively studied, a comprehensive understanding of the mechanisms linking Wnt signalling to other relevant pathways, cell mechanical properties, and cell - cycle progression in health and disease is still lacking.

In this work, we considered how two variations of a previously-proposed Wnt model affect the proliferative dynamics of intestinal crypts. We developed a new multiscale computational model of crypt dynamics, which showed that linking Wnt signalling at the point of cell division (static Wnt), as opposed to continually updating Wnt levels over the cell lifetime (dynamic Wnt), provides a more realistic representation of cell proliferation.

Previous models have assumed the existence of a fixed and externally-imposed gradient of Wnt within the crypt, with a maximal amount of Wnt found at the base, decreasing linearly with height. Based on recent experimental observations, we developed a model that assumes Wnt is internally held by each cell, supplied initially only to cells in a reservoir at the base of the crypt. We showed that subsequent division events create an emergent gradient of Wnt similar to that imposed by

419 existing Wnt models. Noise in the Wnt allocation to daughter cells following mitosis does not
420 significantly affect the overall Wnt gradient, but does smooth the distribution of mitotic activity
421 within the crypt. Increasing the size of the Wnt reservoir controlled the properties of the Wnt gradient,
422 in terms of its steepness and linearity. Furthermore, our results suggest that the spatial localisation of
423 the Wnt reservoir can affect the crypt's dynamics, both wild-type and dysplastic, as much as the total
424 amount of Wnt available.

425 In order to elucidate the mechanisms underpinning cellular CI within the crypt, we extended a
426 Wnt regulatory network model to additionally include the role of Hippo signalling in phosphorylating
427 YAP/TAZ; the latter has been suggested to trap β-catenin within the cytoplasm and at the
428 extracellular matrix, preventing nuclear accumulation and subsequent expression of Wnt target genes
429 linked to cell-cycle progression (59). Our extended regulatory network is sensitive to a reduction in
430 nuclear accumulation of β-catenin; single-cell model simulations showed that Hippo signalling can
431 reduce nuclear β-catenin accumulation, and cause the rapid cessation of the cell cycle, matching
432 experimental observations (35). Agent-based simulations including the Wnt/Hippo signalling
433 coupling, with the levels of Hippo signalling further linked to cell volume, validated the single-cell
434 analysis: the length of the cell cycle increases, and eventually proliferation ceases, as the cell volume
435 decreases. Cells with low Wnt levels are more susceptible to CI; as the level of unphosphorylated β-
436 catenin within the cell is reduced, the amount needed to bind to YAP-P to prevent nuclear
437 accumulation and subsequent transcription of target genes linked to proliferation is reduced.

438 To investigate the effect of mutations within the crypt, we performed agent-based simulations
439 (using both an external-gradient Wnt model with static Wnt, and the internal division-based Wnt
440 model) with an APC double-mutant cell introduced into the crypt. The simulated mutation causes
441 altered destruction complex kinetics in the Wnt signalling, as well as disruption of the Hippo
442 signalling module. Increasing the amount of Wnt within the crypt did not affect the washout
443 probability of the mutant cells at low levels of CI, with the advantage of the mutant cells not
444 significantly reduced by the increase in proliferation caused by Wnt upregulation. The main
445 difference arose from increasing the volume threshold for CI in the cells, with the largest decrease in

446 the washout probability seen at a volume threshold of 90% of the healthy cell equilibrium. The effect
447 on washout probability and cell velocity of this mutant was similar to that of increased adhesion
448 observed previously (44). Critically, moving from the external-gradient to the internally held and
449 division-based Wnt model did not qualitatively affect the increased mutant advantage, further
450 suggesting cell division as a plausible mechanism for the experimentally-observed Wnt gradient (27,
451 46).

452 The results of our study suggest the possibility of combined disease treatment, targeting both
453 the Wnt and Hippo pathways. There are also several possible avenues for further study, to better
454 understand the dynamics of the crypt. In the division-based Wnt model, we assumed a reservoir at the
455 base of the crypt within which cells can uptake Wnt, as a simplification of the presence of Wnt
456 secreting cells at the crypt base. A more detailed model should explicitly consider such cells, and Wnt
457 secretion, in addition to possible uptake from an external reservoir. Our model also simplifies the
458 Hippo-based sequestration of β-catenin within the cell; one worthwhile extension would be to explore
459 the extent to which Hippo signalling either traps β-catenin within the cytoplasm or actively transports
460 it to the extracellular matrix, in turn causing changes to the adhesive behaviour of the cells. Aside
461 from Wnt and Hippo signalling, other processes also play important roles in crypt homeostasis, and
462 would be valuable additions to a more detailed model. For example, the Notch signalling pathway
463 coordinates cell fate specification via interaction with the Wnt pathway (60). More fundamentally,
464 intestinal organoids represent a significant opportunity to investigate crypts *in vitro*; while
465 computational models exist in the literature (43, 47-50), they do not all contain the level of detail
466 described here. By introducing Wnt-secreting cells, and combining them with signalling network
467 dependent cell-cycle models, it could be possible to create a self-sustaining organoid growth model
468 which mimics the *in vivo* dynamics of intestinal crypts.

469

470 **Acknowledgements**

471 LM acknowledges the support of the UK Medical Research Council (MRC, grant MR/N021444/1)
472 and the UK Engineering and Physical Sciences Research Council (EPSRC, grant EP/R041695/1). DW

was supported by an EPSRC Doctoral Training Partnership PhD studentship. AGF is supported by a Vice-Chancellor's Fellowship from the University of Sheffield.

Author Contribution

DW, AGF, MH and LM designed this research; DW implemented the mathematical models, generated simulations, analysed results and prepared the figures; AGF supported agent-based simulations; DW, AGF, MH and LM wrote the manuscript; MH and LM supervised the project. All authors read and approved the final manuscript.

Competing interests

The authors have declared that no competing interests exist.

Methods

The single-cell model combines the subcellular Wnt/Hippo signalling model, as described by a set of 10 Ordinary Differential Equations (ODEs, Figure S1) and the cell-cycle model, which is described by 5 additional ODEs (Figure S2). The signalling model adapts a formalism previously proposed (25, 42) to describe the dynamics of β-catenin and the effects of signalling (Wnt) on the cell-cycle, to further include Hippo-signalling-dependent complex (β-catenin/YAP-P, Equation 10, Figure S1) and its effect on free β-catenin. The cell-cycle model used (both equations and parameters) is as in Swat *et. al.* (22).

The agent-based model was implemented within the Chaste (v. 3.3) modelling framework (52, 53).

Further details about model assumptions, equations, parameters, and simulation settings, can be found in Supplementary Information.

The Chaste project folder for reproducing all agent-based simulations is available at **https://figshare.com/s/5bfa5b61396b29e4641f**

498 **Figure Legends**

499 **Figure 1. Wnt/Hippo signalling network**

500 **(a)** Schematic showing β-catenin cellular localisation, dependent on Wnt and Hippo signalling. β-
501 catenin exists either in the cytosol or in the nucleus, with its localisation directly affecting cell-cycle
502 progression. In the Wnt-Off state (left panel), β-catenin is degraded in the cytosol by a complex
503 comprised of APC, Axin and GSK3, preventing β-catenin nuclear localisation. In the Wnt-On state
504 (right panel), the destruction complex is disrupted by Disheveled (Dsh), resulting in increased β-
505 catenin concentration and its nuclear localisation. This causes the displacement of Groucho in the
506 nucleus and transcription of Wnt target genes linked to proliferation and cell-cycle progression. Hippo
507 signalling causes the phosphorylation of YAP/TAZ within the cytosol. Phosphorylated YAP/TAZ
508 binds to cytosolic β-catenin, preventing its nuclear accumulation and, in turn, transcription of Wnt
509 target genes and cell-cycle progression. **(b)** Network diagram resulting from the schematic in (a) and
510 describing the kinetics within the cell. C_A, C_C, C_T, and C_U are the levels of adhesive-linked β-catenin
511 at the cell surface, cytosolic β-catenin, transcriptional nuclear β-catenin, and β-catenin marked for
512 degradation, respectively. A, T, and D denote the concentrations of molecular species forming
513 complexes with β-catenin at the cell surface (forming adhesive complexes at the adherens junction),
514 within the nucleus, and within the destruction complex, respectively. X and Y denote the
515 concentrations of Axin and transcribed Wnt target proteins, respectively. C_H denotes the concentration
516 of β-catenin/YAP complex formed due to Hippo signalling in the cell. Signalling-dependent rates are
517 indicated by the coloured arrows (yellow for Wnt dependence, pink for Hippo dependence).

518 **Figure 2. Single-cell ODE model of Hippo/Wnt signalling network**

519 **(a)** Single-cell sensitivity analysis of the Hippo signalling module; parameters $\hat{p}_H$ and K_H represent
520 the binding and dissociation rates of phosphorylated YAP/β-catenin and its complex, respectively.
521 The coloured region shows the length of the cell cycle, and the white region represents cell-cycle
522 cessation. **(b)** Single-cell sensitivity analysis of the Hippo-dependent cell cycle as a function of (static
523 input) Wnt level and $\hat{p}_H$. **(c)** Schematic diagram of the 3D to 2D projection method, 'unrolling' the

524 cylindrical crypt to a planar domain with periodic boundary conditions. The right panel illustrates the
525 imposed-gradient Wnt model M1, in the two considered cases of minimum Wnt level at 40% and
526 100% of the height of the crypt, and the resultant effect on cell proliferation region.

527 **Figure 3. Multiscale dynamics of Hippo and Wnt signalling, and Hippo-dependent contact-**
528 **inhibition (CI), in wild type crypt with imposed Wnt gradient (M1)**

529 **(a, b)** Effects of Hippo signalling-based CI on Wnt signalling-dependent cell cycle measuring mitotic
530 indices (proportion of cells undergoing mitosis as a function of position in the crypt). We considered
531 both static (M1a, solid lines) and dynamic (M2a, dashed lines) Wnt cell models (Wnt assigned at birth
532 or continually updated, respectively), with Wnt signalling affecting 100% (a) or 40% (b) of the crypt.
533 The different volumes at which cells undergo CI are indicated by red lines (CI at 60% of equilibrium
534 volume) and blue lines (CI at 90% of equilibrium volume). **(c, d)** Velocity whisker plots for a crypt
535 cell population using the static (M1a) Wnt model, and Wnt signalling affecting 100% (c) or 40% (d)
536 of the crypt. The box plots indicate the median velocity of the cells at increasing heights up the crypt,
537 with the box representing the 25th and 75th percentiles respectively. The whiskers extend to the most
538 extreme velocities recorded over the course of the 150 repeated experiments**.**

539 **Figure 4. Multiscale crypt dynamics using a cell division-based Wnt model (M2)**

540 **(a, b)** Wnt gradient through the crypt for the cell division-based Wnt model (M2), with (a) 10%, and
541 (b) 20% crypt-height Wnt reservoir. **(c, d)** Mitotic activity, with asymmetric division of Wnt between
542 daughter cells in crypts with (c) 10% and (d) 20% crypt-height Wnt reservoir; blue, red and green
543 lines represent symmetric division, 5% and 10% noise, respectively. The shaded regions show the
544 resultant standard deviation across the repeated experiments.

545 **Figure 5. Washout probabilities upon mis-regulated Wnt and Hippo signalling activity**

546 **(a, b)** Washout probabilities for APC double-mutant crypt, starting from a single mutant cell
547 introduced at the base of the crypt using (a) externally-imposed gradient (M1a) or (b) cell-division
548 based (M2) Wnt models. Red and blue lines represent the low (40% Wnt threshold/10% Wnt
549 reservoir) and high (100% Wnt threshold/20% Wnt reservoir) Wnt cases, respectively. Increasing the

550 threshold for CI reduces the probability of mutant washout. Shaded regions represent 95% confidence
551 intervals.

552

553 **References**

554 1. Ferlay J, Soerjomataram I, Dikshit R, Eser S, Mathers C, Rebelo M, et al. Cancer incidence
555 and mortality worldwide: Sources, methods and major patterns in GLOBOCAN 2012. International
556 Journal of Cancer. 2015.
557 2. Bosetti C, Levi F, Rosato V, Bertuccio P, Lucchini F, Negri E, et al. Recent trends in
558 colorectal cancer mortality in Europe. Int J Cancer. 2011;129(1):180-91.
559 3. Young M, Ordonez L, Clarke AR. What are the best routes to effectively model human
560 colorectal cancer? Mol Oncol. 2013;7(2):178-89.
561 4. Baker AM, Cereser B, Melton S, Fletcher AG, Rodriguez-Justo M, Tadrous PJ, et al.
562 Quantification of crypt and stem cell evolution in the normal and neoplastic human colon. Cell
563 Reports. 2014;8(4):940-7.
564 5. Dunn S-J, Osborne JM, Appleton PL, Näthke I. Combined changes in Wnt signaling response
565 and contact inhibition induce altered proliferation in radiation-treated intestinal crypts. Molecular
566 Biology of the Cell. 2016;27:1863-74.
567 6. Trani D, Nelson SA, Moon B-H, Swedlow JJ, Williams EM, Strawn SJ, et al. High-Energy
568 Particle-Induced Tumorigenesis Throughout the Gastrointestinal Tract. Radiation Research.
569 2014;181(2):162-71.
570 7. Potten CS, Kellett M, Rew DA, Roberts SA. Proliferation in human gastrointesinal epithelium
571 using bromodeoxyuridine in vivo: Data for different sites, proximity to a tumour, and polyposis coli.
572 Gut. 1992;33(4):524-9.
573 8. Sunter JP, Appleton DR, Dé Rodriguez MS, Wright Na, Watson AJ, De Rodriguez MS. A
574 comparison of cell proliferation at different sites within the large bowel of the mouse. Journal of
575 anatomy. 1979;129:833-42.
576 9. Stamos JL, Weis WI. The β-catenin destruction complex. Cold Spring Harbor Perspectives in
577 Biology. 2013;5(1).
578 10. Reya T, Clevers H. Wnt signalling in stem cells and cancer. Nature. 2005;434(7035):843-50.
579 11. Ilyas M. Wnt signalling and the mechanistic basis of tumour development. Journal of
580 Pathology. 2005;205(2):130-44.
581 12. Lloyd-Lewis B, Fletcher AG, Dale TC, Byrne HM. Toward a quantitative understanding of
582 the Wnt/β-catenin pathway through simulation and experiment. Wiley Interdisciplinary Reviews:
583 Systems Biology and Medicine. 2013;5(4):391-407.

584 13. Sumigray KD, Terwilliger M, Lechler T. Morphogenesis and Compartmentalization of the
585 Intestinal Crypt. Developmental Cell. 2018;45(2):183-97.
586 14. Van de Wetering M, Sancho E, Verweij C, De Lau W, Oving I, Hurlstone A, et al. The β-
587 catenin/TCF-4 complex imposes a crypt progenitor phenotype on colorectal cancer cells. Cell.
588 2002;111:241-50.
589 15. Clevers H, Nusse R. Wnt/β-catenin signaling and disease. Cell. 2012;149(6):1192-205.
590 16. Potten CS, Kellett M, Roberts SA, Rew DA, Wilson GD. Measurement of in vivo
591 proliferation in human colorectal mucosa using bromodeoxyuridine. Gut. 1992;33(1):71-8.
592 17. Kwong LN, Dove WF. APC and its modifiers in colon cancer. Advances in experimental
593 medicine and biology. 2009;656:85-106.
594 18. Lamlum H, Papadopoulou A, Ilyas M, Rowan A, Gillet C, Hanby A, et al. APC mutations are
595 sufficient for the growth of early colorectal adenomas. Proceedings of the National Academy of
596 Sciences. 2000;97(5):2225-8.
597 19. Fre S, Huyghe M, Mourikis P, Robine S, Louvard D, Artavanis-Tsakonas S. Notch signals
598 control the fate of immature progenitor cells in the intestine. Nature. 2005;435:964-8.
599 20. Wright NAA, Malcolm. The biology of epithelial cell populations. Oxford: Oxford University
600 Press; 1984.
601 21. Varelas X, Miller BW, Sopko R, Song S, Gregorieff A, Fellouse FA, et al. The Hippo
602 Pathway Regulates Wnt/β-Catenin Signaling. Developmental Cell. 2010;18:579-91.
603 22. Swat M, Kel A, Herzel H. Bifurcation analysis of the regulatory modules of the mammalian
604 G 1 / S transition. Bioinformatics. 2004;20:1506-11.
605 23. Scoville DH, Sato T, He XC, Li L. Current View: Intestinal Stem Cells and Signaling.
606 Gastroenterology. 2008;134(3):849-64.
607 24. Mirams GR, Fletcher AG, Maini PK, Byrne HM. A theoretical investigation of the effect of
608 proliferation and adhesion on monoclonal conversion in the colonic crypt. Journal of Theoretical
609 Biology. 2012;312:143-56.
610 25. van Leeuwen IMM, Mirams GR, Walter A, Fletcher AG, Murray PJ, Osborne J, et al. An
611 integrative computational model for intestinal tissue renewal. Cell Proliferation. 2009;42:617-36.
612 26. Ingham-Dempster T, Corfe B, Walker D. A cellular based model of the colon crypt suggests
613 novel effects for Apc phenotype in colorectal carcinogenesis. J Comput Sci-Neth. 2018;24:125-31.
614 27. Farin HF, Jordens I, Mosa MH, Basak O, Korving J, Tauriello DV, et al. Visualization of a
615 short-range Wnt gradient in the intestinal stem-cell niche. Nature. 2016;530(7590):340-3.
616 28. Dong J, Feldmann G, Huang J, Wu S, Zhang N, Comerford SA, et al. Elucidation of a
617 Universal Size-Control Mechanism in Drosophila and Mammals. Cell. 2007;130:1120-33.
618 29. Helmlinger G, Netti PA, Lichtenbeld HC, Melder RJ, Jain RK. Solid stress inhibits the
619 growth of multicellular tumor spheroids. Nature Biotechnology. 1997;15:778-83.

620 30. Eisenhoffer GT, Loftus PD, Yoshigi M, Otsuna H, Chien CB, Morcos PA, et al. Crowding
621 induces live cell extrusion to maintain homeostatic cell numbers in epithelia. Nature.
622 2012;484(7395):546-9.
623 31. Zeng Q, Hong W. The Emerging Role of the Hippo Pathway in Cell Contact Inhibition,
624 Organ Size Control, and Cancer Development in Mammals. Cancer Cell. 2008;13(3):188-92.
625 32. Zhao B, Zhao B, Wei X, Wei X, Li W, Li W, et al. Inactivation of YAP oncoprotein by the
626 Hippo pathway is involved in cell contact inhibition and tissue growth control. Genes & development.
627 2007;21:2747-61.
628 33. Camargo FD, Gokhale S, Johnnidis JB, Fu D, Bell GW, Jaenisch R, et al. YAP1 Increases
629 Organ Size and Expands Undifferentiated Progenitor Cells. Current Biology. 2007;17:2054-60.
630 34. Barry ER, Camargo FD. The Hippo superhighway: Signaling crossroads converging on the
631 Hippo/Yap pathway in stem cells and development. Current Opinion in Cell Biology. 2013;25:247-
632 53.
633 35. Imajo M, Miyatake K, Iimura A, Miyamoto A, Nishida E. A molecular mechanism that links
634 Hippo signalling to the inhibition of Wnt/β-catenin signalling. EMBO Journal. 2012;31:1109-22.
635 36. Dupont S, Morsut L, Aragona M, Enzo E, Giulitti S, Cordenonsi M, et al. Role of YAP/TAZ
636 in mechanotransduction. Nature. 2011;474:179-84.
637 37. Jaalouk DE, Lammerding J. Mechanotransduction gone awry. Nature Reviews Molecular Cell
638 Biology. 2009;10(1):63-73.
639 38. Johnson R, Halder G. The two faces of Hippo: targeting the Hippo pathway for regenerative
640 medicine and cancer treatment. Nature Reviews Drug Discovery. 2013;13:63-79.
641 39. Yang C-C, Graves HK, Moya IM, Tao C, Hamaratoglu F, Gladden AB, et al. Differential
642 regulation of the Hippo pathway by adherens junctions and apical–basal cell polarity modules.
643 Proceedings of the National Academy of Sciences. 2015;112:1785-90.
644 40. Schroeder MC, Halder G. Regulation of the Hippo pathway by cell architecture and
645 mechanical signals. Seminars in Cell and Developmental Biology. 2012;23(7):803-11.
646 41. Piccolo S, Dupont S, Cordenonsi M. The Biology of YAP/TAZ: Hippo Signaling and
647 Beyond. Physiological Reviews. 2014;94:1287-312.
648 42. van Leeuwen IMM, Byrne HM, Jensen OE, King JR. Elucidating the interactions between the
649 adhesive and transcriptional functions of β-catenin in normal and cancerous cells. Journal of
650 Theoretical Biology. 2007;247:77-102.
651 43. Fletcher AGM, Phillip.; Maini, Phillip. Multiscale modelling of intestinal crypt organization
652 and carcinogenesis. Mathematical Models and Methods in Applied Sciences. 2015;484:546-9.
653 44. Fletcher AG, Breward CJW, Jonathan Chapman S. Mathematical modeling of monoclonal
654 conversion in the colonic crypt. Journal of Theoretical Biology. 2012;300:118-33.

655 45. Farin HF, Van Es JH, Clevers H. Redundant sources of Wnt regulate intestinal stem cells and
656 promote formation of paneth cells. Gastroenterology. 2012;143(6):1518-29.
657 46. Shoshkes-Carmel M, Wang YJ, Wangensteen KJ, Tóth B, Kondo A, Massassa EE, et al.
658 Subepithelial telocytes are an important source of Wnts that supports intestinal crypts. Nature.
659 2018;557(7704):242-6.
660 47. Lee E, Salic A, Krüger R, Heinrich R, Kirschner MW. The roles of APC and axin derived
661 from experimental and theoretical analysis of the Wnt pathway. PLoS Biology. 2003;1(1):116-32.
662 48. Mirams GR, Byrne HM, King JR. A multiple timescale analysis of a mathematical model of
663 the Wnt/beta-catenin signalling pathway. Journal of mathematical biology. 2010;60(1):131-60.
664 49. Schmitz Y, Rateitschak K, Wolkenhauer O. Analysing the impact of nucleo-cytoplasmic
665 shuttling of β-catenin and its antagonists APC, Axin and GSK3 on Wnt/β-catenin signalling. Cellular
666 Signalling. 2013;25(11):2210-21.
667 50. MacLean AL, Rosen Z, Byrne HM, Harrington HA. Parameter-free methods distinguish Wnt
668 pathway models and guide design of experiments. Proceedings of the National Academy of Sciences.
669 2015;112(9):2652-7.
670 51. Pedone E, Olteanu V-A, Marucci L, Muñoz-Martin MI, Youssef SA, de Bruin A, et al.
671 Modeling Dynamics and Function of Bone Marrow Cells in Mouse Liver Regeneration. Cell Reports.
672 2017;18(1):107-21.
673 52. Pitt-Francis J, Pathmanathan P, Bernabeu MO, Bordas R, Cooper J, Fletcher AG, et al.
674 Chaste: A test-driven approach to software development for biological modelling. Computer Physics
675 Communications. 2009;180:2452-71.
676 53. Mirams GR, Arthurs CJ, Bernabeu MO, Bordas R, Cooper J, Corrias A, et al. Chaste: An
677 Open Source C++ Library for Computational Physiology and Biology. PLoS Computational Biology.
678 2013;9.
679 54. Dunn SJ, Fletcher AG, Chapman SJ, Gavaghan DJ, Osborne JM. Modelling the role of the
680 basement membrane beneath a growing epithelial monolayer. Journal of Theoretical Biology.
681 2012;298:82-91.
682 55. Osborne JM, Fletcher AG, Pitt-Francis JM, Maini PK, Gavaghan DJ. Comparing individual-
683 based approaches to modelling the self-organization of multicellular tissues. PLoS Computational
684 Biology. 2017;13(2):e1005387.
685 56. Godwin S, Ward D, Pedone E, Homer M, Fletcher AG, Marucci L. An extended model for
686 culture-dependent heterogenous gene expression and proliferation dynamics in mouse embryonic
687 stem cells. NPJ Syst Biol Appl. 2017;3:19.
688 57. Qu Y, Gharbi N, Yuan X, Olsen JR, Blicher P, Dalhus B, et al. Axitinib blocks Wnt/β-catenin
689 signaling and directs asymmetric cell division in cancer. Proceedings of the National Academy of
690 Sciences. 2016;113(33):9339-44.

691 58. Cai J, Maitra A, Anders Ra, Taketo MM, Pan D. β -Catenin destruction complex-
692 independent regulation of Hippo – YAP signaling by APC in intestinal tumorigenesis. Genes &
693 development. 2015:1-14.
694 59. Miyaoka Y, Miyajima A. To divide or not to divide: Revisiting liver regeneration. Cell
695 Division. 2013;8(1):8.
696 60. Kay SK, Harrington HA, Shepherd S, Brennan K, Dale T, Osborne JM, et al. The role of the
697 Hes1 crosstalk hub in Notch-Wnt interactions of the intestinal crypt. PLoS Computational Biology.
698 2017;13(2):e1005400.
699

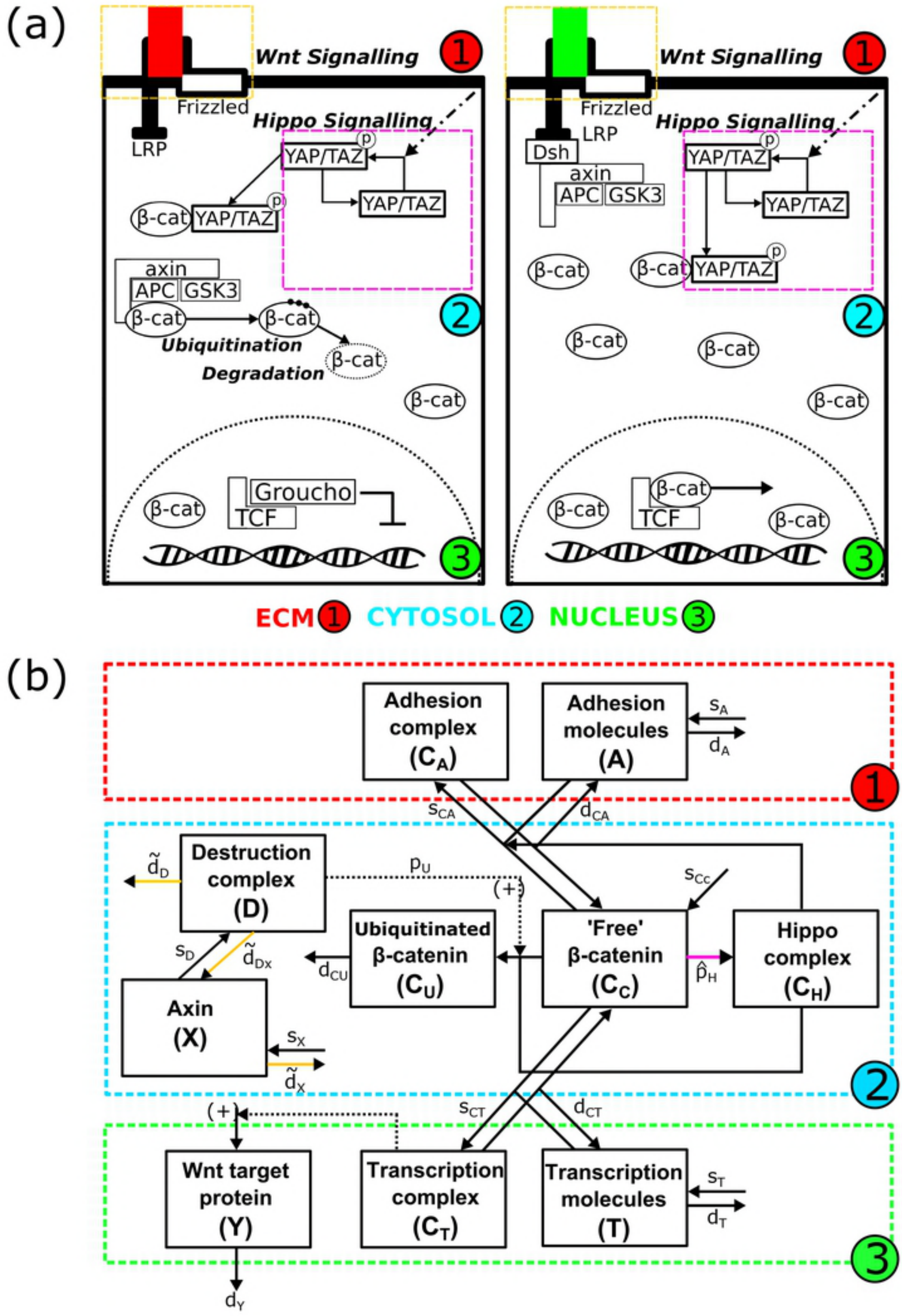

Figure 1.

Figure 1

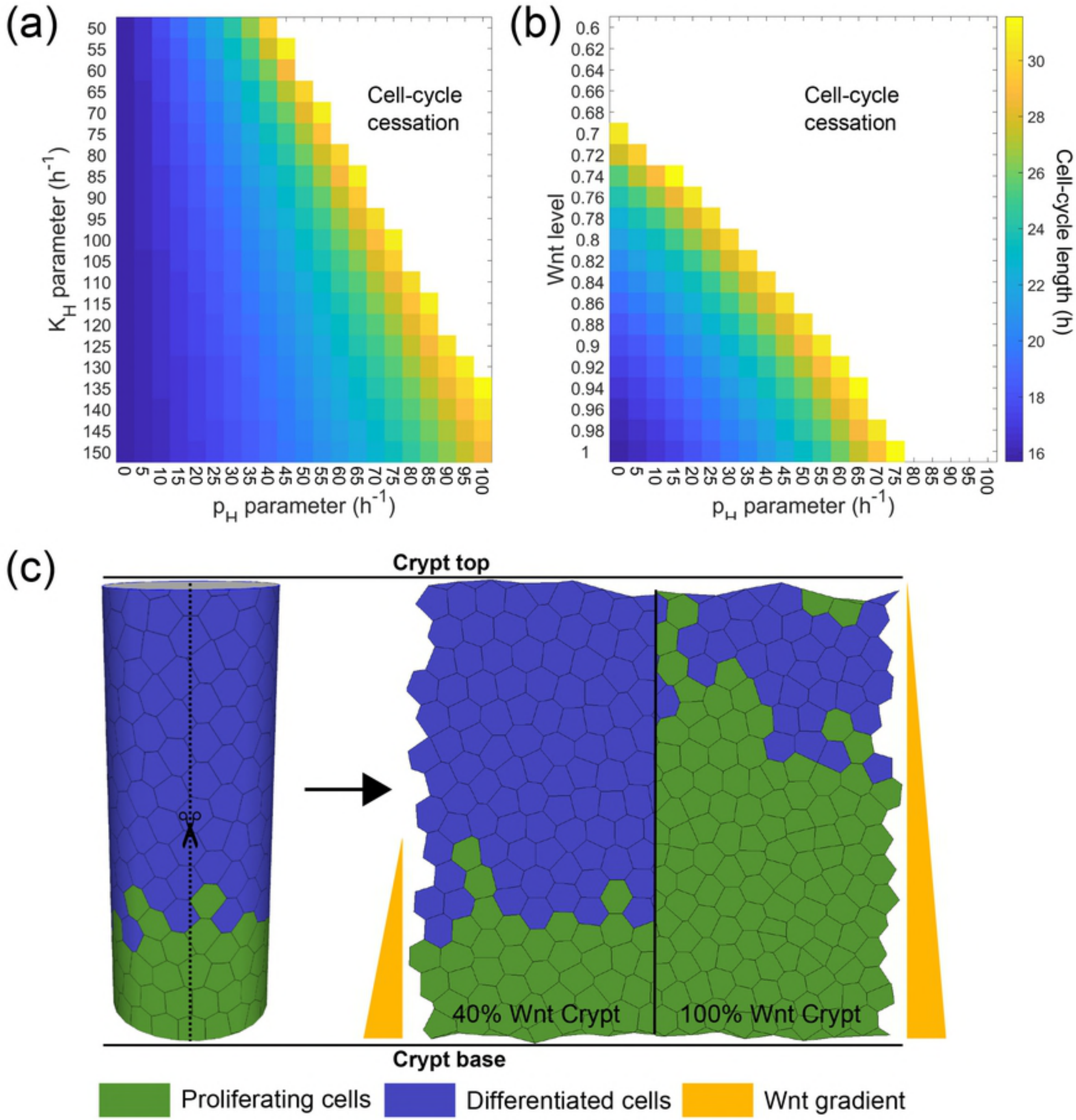

Figure 2.

Figure 2

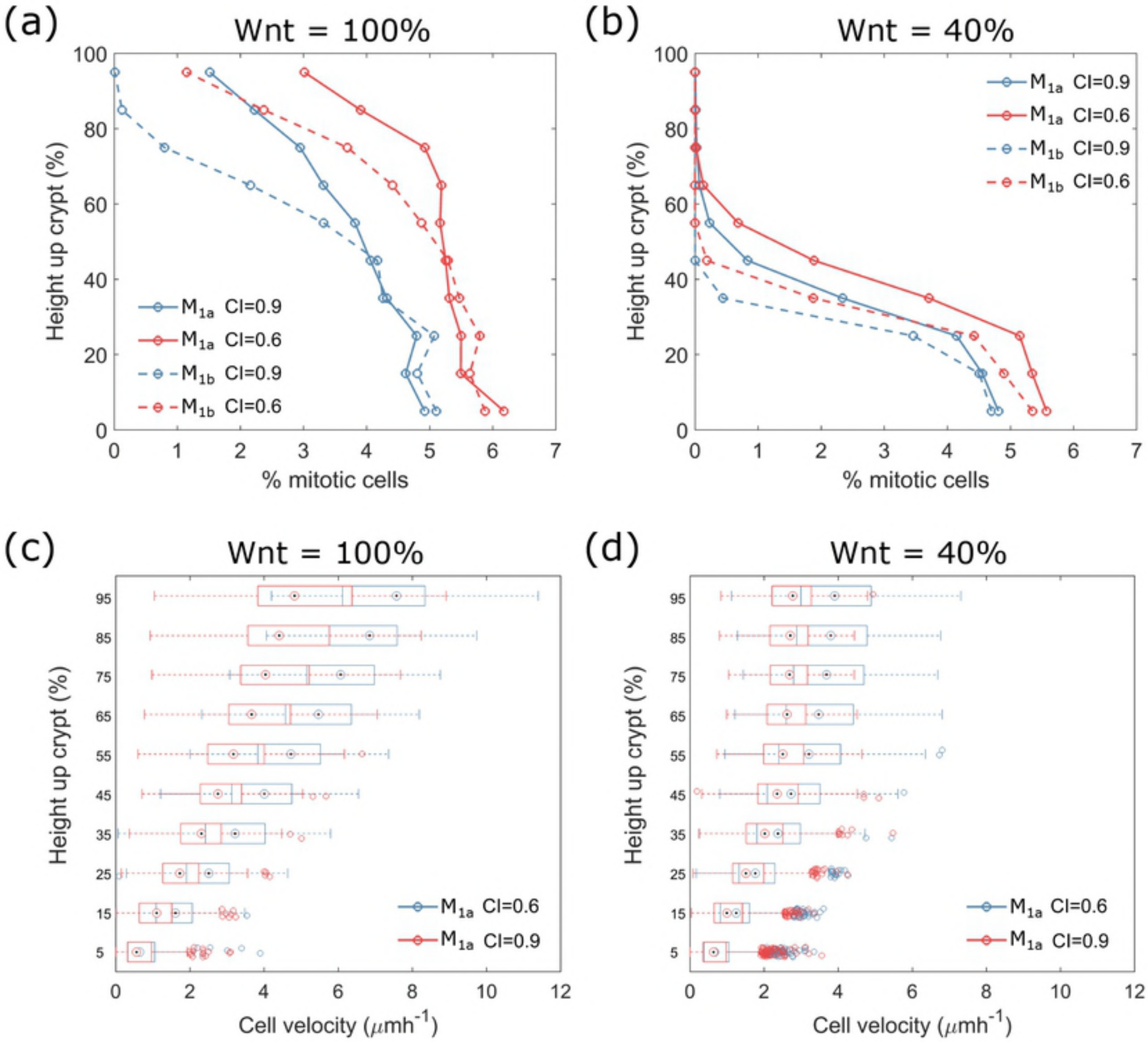

Figure 3.

Figure 3

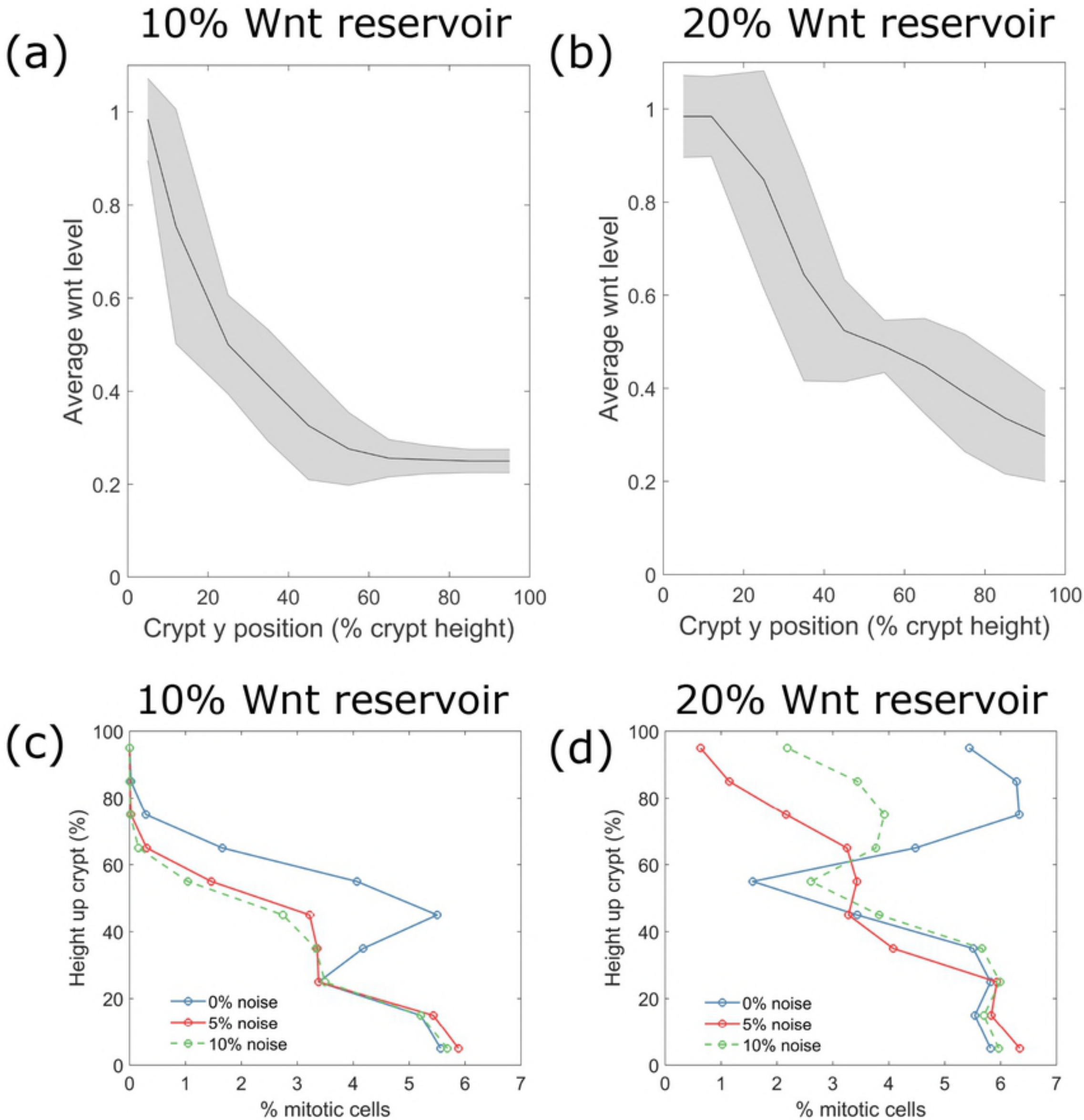

Figure 4.

Figure 4

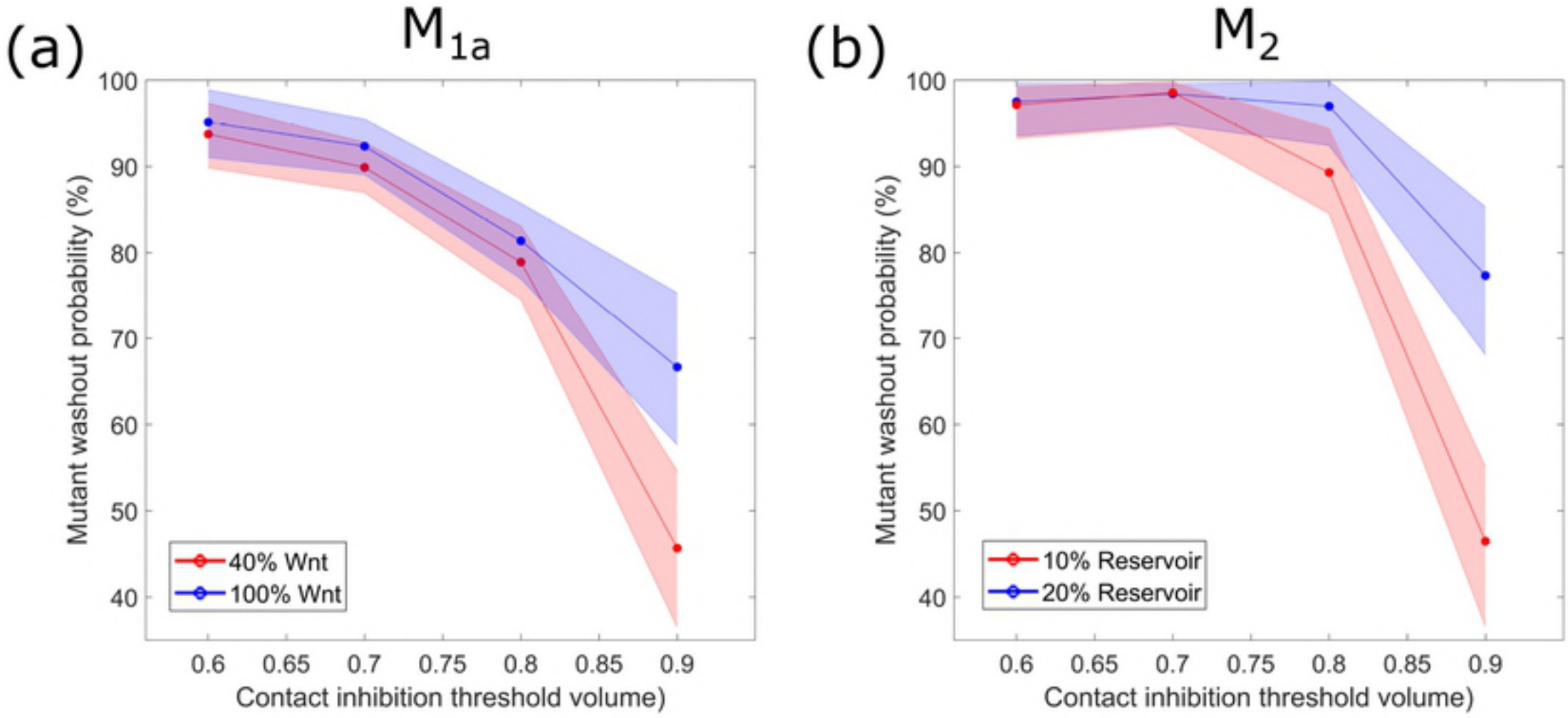

Figure 5.

Figure 5